

Supplemental Material:

Supplemental Materials and Methods

Immunofluorescence

Immunostaining of ovaries, S2 cells and OSCs was performed as previously described (Saito et al. 2006; Saito et al. 2009). The primary antibodies used were: culture supernatants of anti-Armi hybridoma cells (1:1 dilution), culture supernatants of anti-Piwi hybridoma cells (P4D2; 1:1 dilution) (Saito et al. 2006), a mouse monoclonal antibody for the myc-tag (1:1,000 dilution; Sigma), a guinea pig antibody against TJ (1:2,000 dilution) (Li et al. 2003) and a rabbit polyclonal antibody against Yb (1:250 dilution) (Szakmary et al. 2009). The secondary antibodies used were: Alexa 488-conjugated anti-mouse IgG (Molecular Probes), Alexa 546-conjugated anti-mouse IgG (Invitrogen), Alexa 488-conjugated anti-rabbit IgG (Invitrogen), Alexa 546-conjugated anti-guinea pig IgG (Invitrogen) and Alexa 546-conjugated anti-rabbit IgG (Invitrogen). DNA was stained with 4',6-diamidino-2-phenylindole (DAPI). Before fixation, the cells were incubated with MitoTracker Orange CMXRos (Invitrogen) targeted at the active mitochondria in living cells. All images were collected using a confocal microscope (Zeiss LSM5 EXCITER; Zeiss).

Immunoprecipitation

Immunoprecipitation from S2 lysates was performed essentially as previously described (Miyoshi et al. 2005). Immunoprecipitation from OSCs was also performed essentially

as previously described (Saito et al. 2009). Briefly, 1×10^8 OSCs were homogenized in homogenization buffer [20 mM HEPES-KOH (pH7.3), 2 mM $MgCl_2$, 1 mM dithiothreitol (DTT), 150 mM NaCl, 2 μ g/ml pepstatin, 2 μ g/ml leupeptin, 0.5% aprotinin and 0.1% NP-40] to prepare OSC lysates. Anti-Piwi (P3G11) (Saito et al. 2006), anti-Armi and anti-Yb (Szakmary et al. 2009) antibodies were immobilized on Dynabeads protein G (Invitrogen). Reaction mixtures were rocked at 4°C for 2 h and the beads were washed four times with homogenization buffer. Total RNAs were isolated from the immunoprecipitates with phenol-chloroform and were precipitated with ethanol. RNAs were dephosphorylated with calf intestinal phosphatase (TaKaRa) and labeled with ^{32}P -gATP using T4 PNK (TaKaRa) for visualization.

Analysis of piRNA-intermediate chemical structures

Total RNAs were isolated from the anti-Armi immunoprecipitates. Phosphorylation of RNAs was performed in the presence of 1 mM ATP with T4 PNK (NEB). Alkaline dephosphorylation was performed with calf intestinal phosphatase (NEB). Acidic dephosphorylation was carried out with T4 PNK (Takara) in 50 mM Tris-HCl (pH 6.5), 10 mM $MgCl_2$ and 5mM DTT. Enzymes were inactivated by phenol/chloroform extraction, followed by RNA precipitation. Precipitates were dissolved in H_2O . Polyadenylation was performed with poly (A) polymerase (NEB) and 1 mM ATP in 1 \times poly (A) polymerase reaction buffer. RNAs were resolved on a 12% denaturing polyacrylamide gel and blotted on Hybond N+ (GE Healthcare) or Hybond N (GE Healthcare) membrane. To cross-link RNAs, UV irradiation or EDC reagent was used.

Drosophila strains

Yellow white (*y w*) and Oregon R were employed as WT strains. The *armi* alleles used were *armi*^{72.1} and *armi*^l (Cook et al. 2004). All stocks were maintained at 25°C.

myc-Piwi expression and RNAi in OSCs

To yield RNAi-resistant *piwi* cDNA (Piwi-r), 5' and 3' fragments of *piwi* cDNA were individually amplified by KOD plus DNA polymerase (Toyobo) using the following primers: 5' fragment, Piwi-F and Piwi-mt-R; 3' fragment, Piwi-mt-F and Piwi-R (primers are listed in Supplemental Table S2). To yield Piwi PAZ mutant cDNA (myc-Piwi-PAZmt), 5' and 3' fragments of *piwi* cDNA were individually amplified by KOD plus DNA polymerase (Toyobo) using the following primers: 5' fragment, Piwi-F and Piwi-PAZmt-R; 3' fragment, Piwi-PAZmt-F and Piwi-R (primers are shown in Table S2). The resulting DNA fragments were gel-purified, mixed and used as templates for PCR amplification. DNA fragments were amplified by PCR with Piwi-F and Piwi-R. The resulting PCR products were cloned into the pAcM vector (Saito et al. 2009) and the sequence was validated by DNA sequence analysis. A short DNA fragment encoding a myc-tag was inserted between the *Xho* I and *Bam* HI sites of pAcM to produce pAcM-Myc. Full-length *zuc* cDNA was inserted between the *Nhe* I and *Xho* I sites of pAcM-Myc to yield pAc-Zuc-myc. For RNAi and expressing myc-tagged proteins in OSCs, trypsinized OSCs (3×10^6 cells) were suspended in 100 µl of Solution V of the Cell Line Nucleofector Kit V (Amaxa Biosystems) together with

either 200 pmol of siRNA duplex or 5 µg of plasmid vector. Transfection was conducted in electroporation cuvettes using a Nucleofector device (Amaxa Biosystems). The transfected cells were transferred to fresh OSC medium and incubated at 26°C for 2 d for further experiments. The siRNAs utilized for RNAi are summarized in Table S2. The control siRNA was enhanced green fluorescent protein (*EGFP*) siRNA (Saito et al. 2009). Quantitative RT-PCR was performed as previously described (Kawamura et al. 2008). Total RNA (0.5 µg) was used to reverse transcribe target sequences using oligo(dT) primer. The resulting cDNA was analyzed by quantitative RT-PCR using a LightCycler real-time PCR system (Roche Diagnostics) using SYBR Premix Ex Taq (Takara). Relative steady-state mRNA levels were determined from the threshold cycle for amplification. Table S2 lists the PCR primer sequences. Ribosomal protein 49 (*Rp49*) was used as an internal control.

Cloning of small RNAs and processing sequence tags

Armi was immunopurified from OSCs using a specific antibody. After immunoprecipitation, total RNAs were isolated from the anti-Armi immunoprecipitates. Acidic dephosphorylation was carried out with T4 PNK (Takara) in 50 mM Tris-HCl (pH 6.5), 10 mM MgCl₂ and 5mM DTT. Enzymes were inactivated by phenol/chloroform extraction, followed by RNA precipitation. Precipitates were dissolved in H₂O. RNAs were resolved on a 12% denaturing polyacrylamide gel with 5'-labelled Decade Marker (Ambion) as a size marker. RNAs of 50-75 nt were excised from the gel. Cloning of RNAs was carried out as described previously (Saito et al.

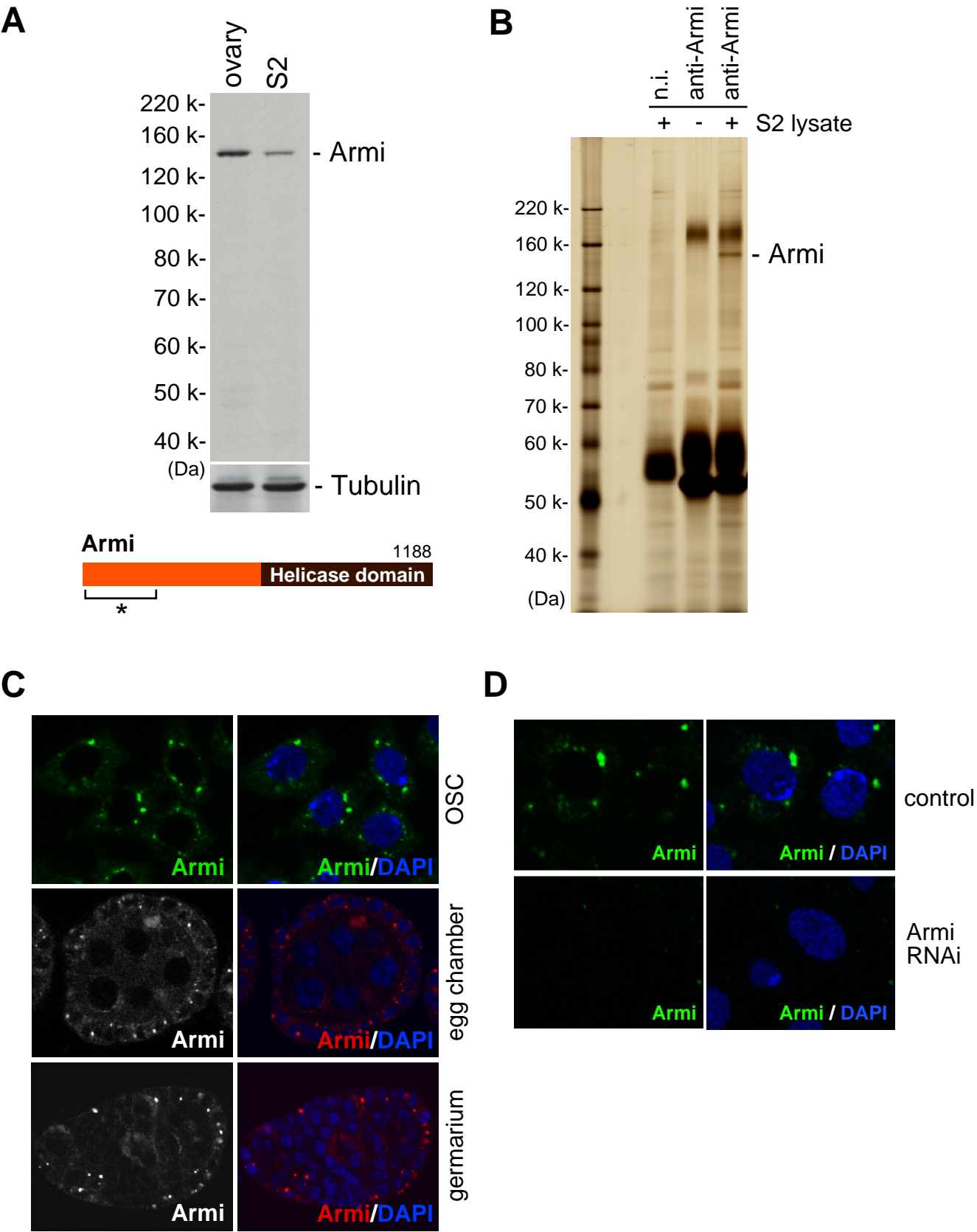
2009). The sequencing was performed on a GS FLX system (Roche).

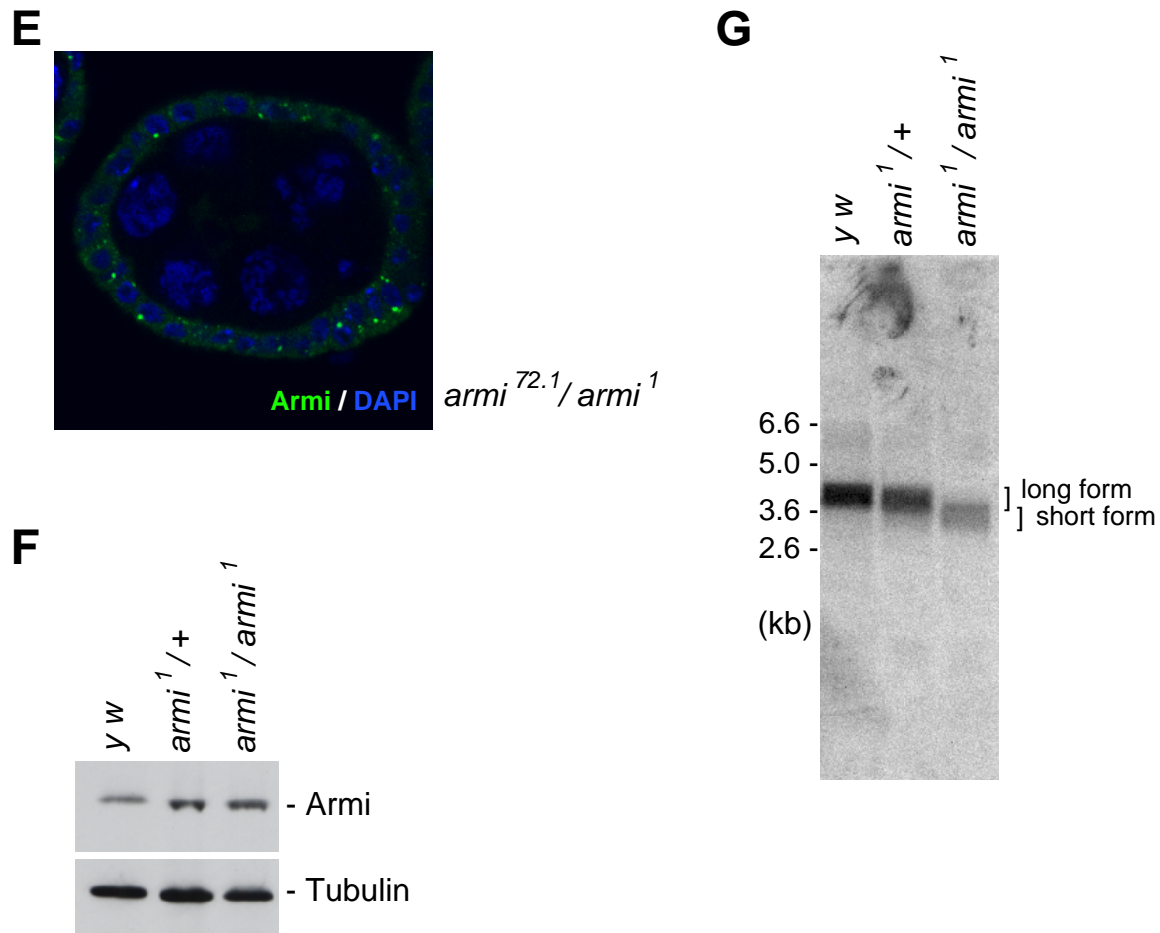
Genome mapping, annotation and frequency mapping

We followed a previously described procedure to map and annotate sequences (Saito et al. 2009). We mapped 116,680 piR-IL sequences to the *Drosophila melanogaster* (dm3) genome. The annotation results are shown as a pie-chart in Supplemental Fig. S4A. Maps for piL-ILs were generated (Supplemental Fig. S5 and S6A), representing the number of piR-ILs that are 100% identical to the genomic sequence. RNA sequences of piR-ILs have been deposited at the GEO database under accession number GSE23931.

Northern blotting

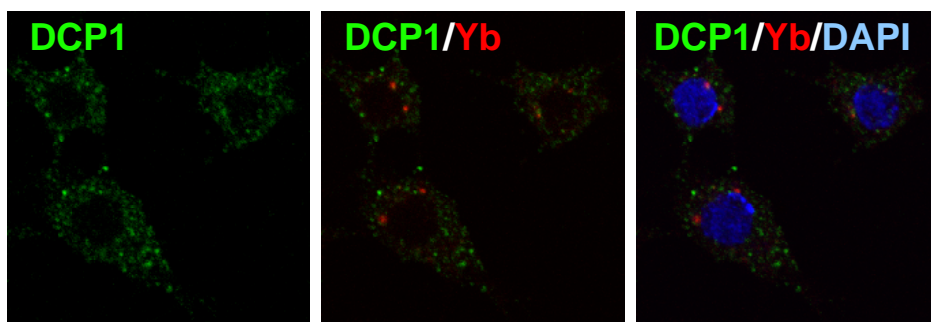
Northern blotting was performed as previously described (Saito et al. 2006). DNA oligonucleotides used are summarized in Table S2.



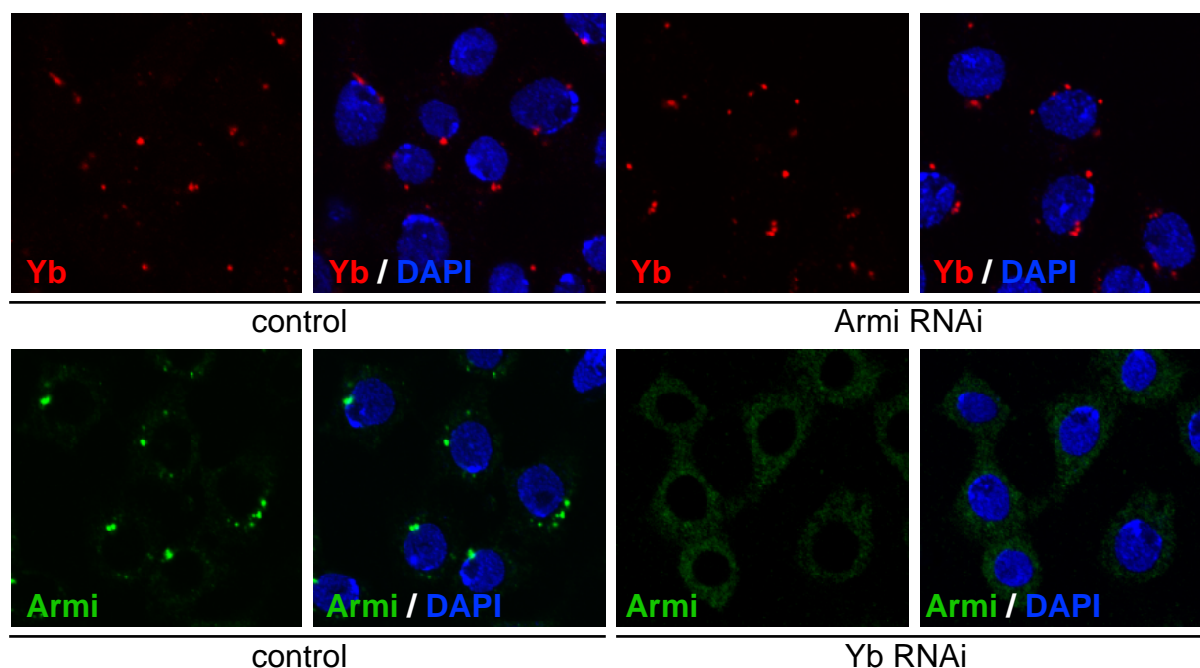


Supplemental Figure S1. (A) Western blot analyses on ovary and S2 cell lysates using anti-Armi antibodies. Anti-tubulin was utilized as an internal control. The antigen (the N-terminal end of Armi; aa 1-200; indicated as *) used for immunizing mice is shown at the bottom. (B) Immunoprecipitation was performed from S2 cells using anti-Armi antibodies. Mass spectrometric analysis determined that the ~150 kDa protein is Armi. (C) Immunofluorescence of Armi in OSCs and ovaries. DAPI staining (blue) shows the locations of the nuclei. (D) Immunostaining of OSCs before and after the treatment with RNAi for Armi indicates that the dotted signals in the cytoplasm reflect the subcellular localization of Armi in the cells. (E) Immunostaining pattern of Armi in the *armi* transheterozygous mutant ovary. (F) Western blot analysis shows that Armi is expressed even in the *armi* homozygous mutant ovaries. (G) Northern blotting shows that the *armi* transcripts (short form) are expressed in the *armi* homozygous mutant ovaries.

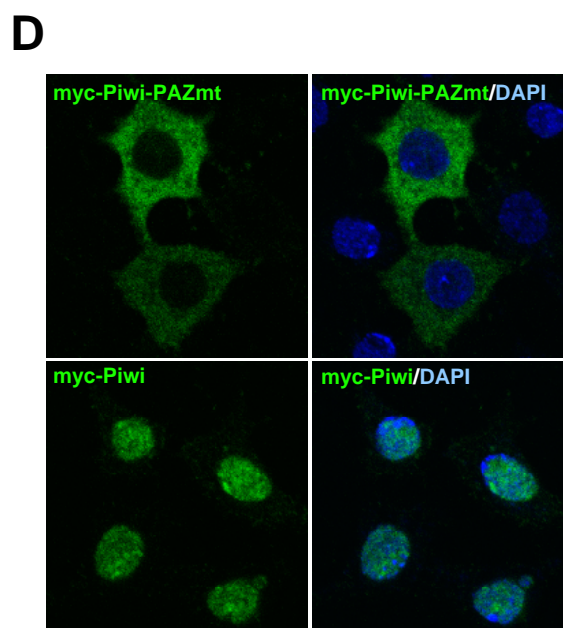
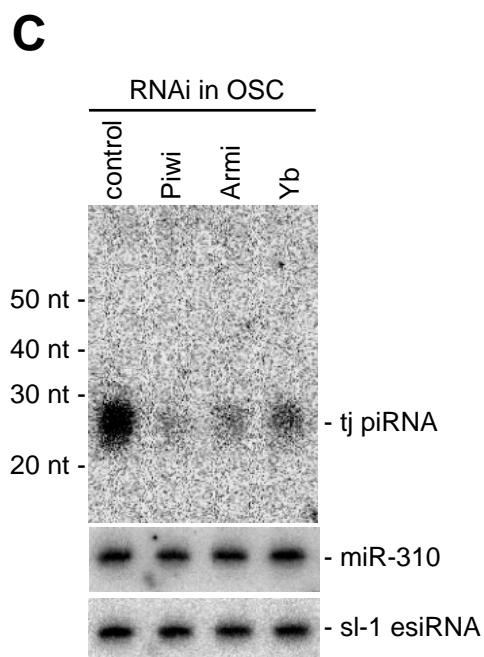
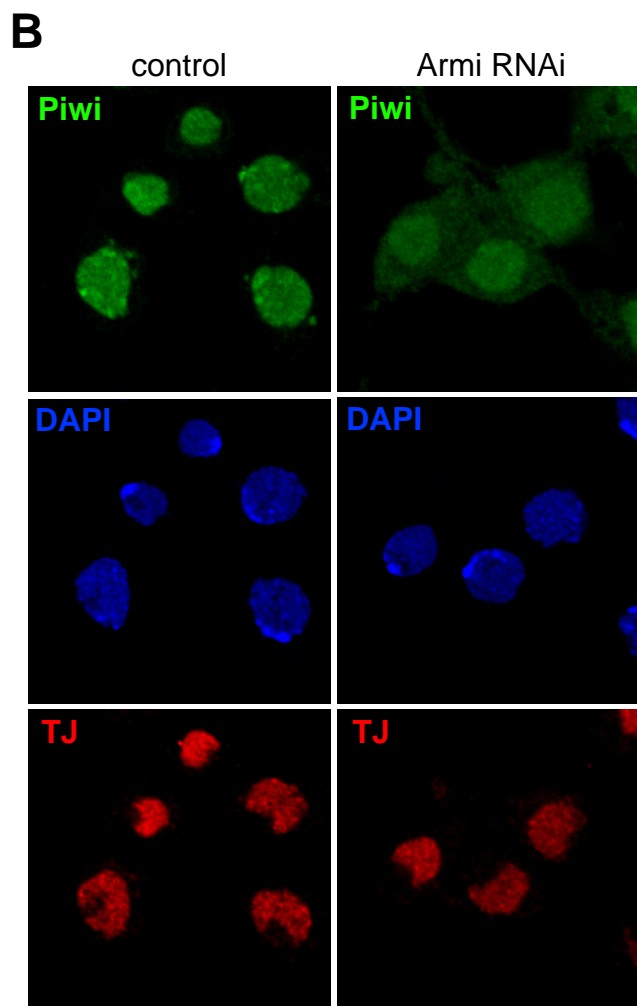
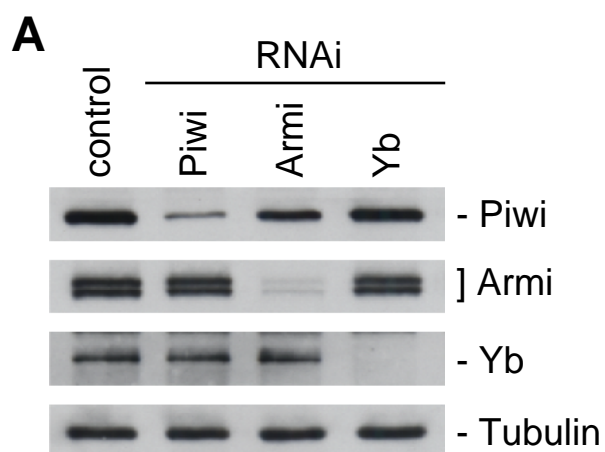
A



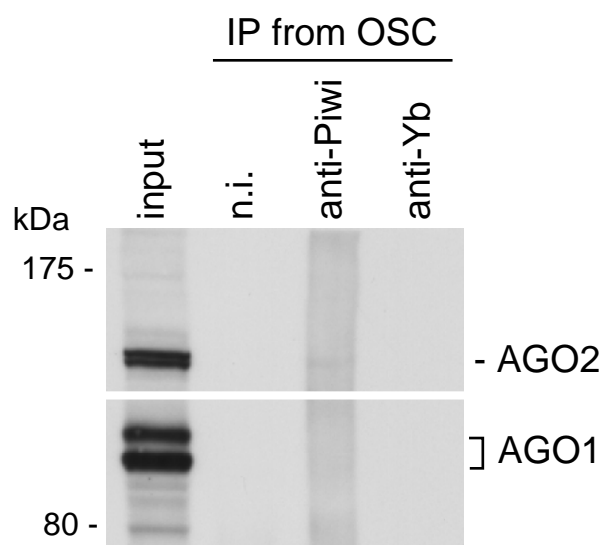
B



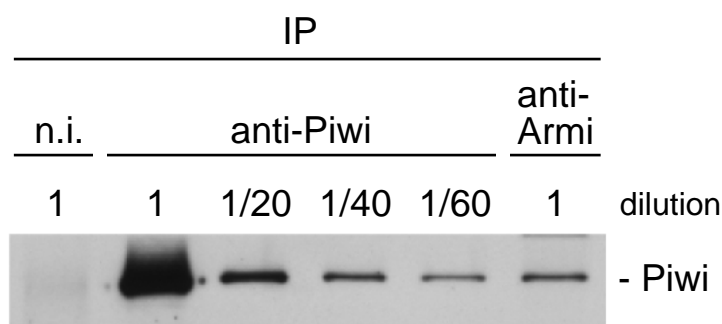
Supplemental Figure S2. (A) Coimmunostaining of OSCs with anti-Yb and anti-Dcp1 antibodies shows that Yb bodies do not colocalize with P bodies. (B) Depletion of Armi did not affect the cellular localization of Yb whereas depletion of Yb caused Armi to be localized to the cytoplasm.



E

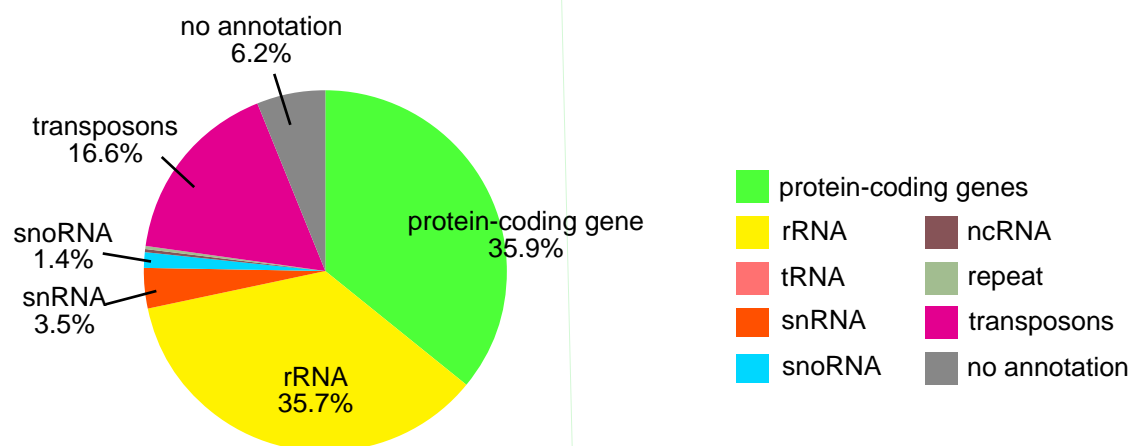


F

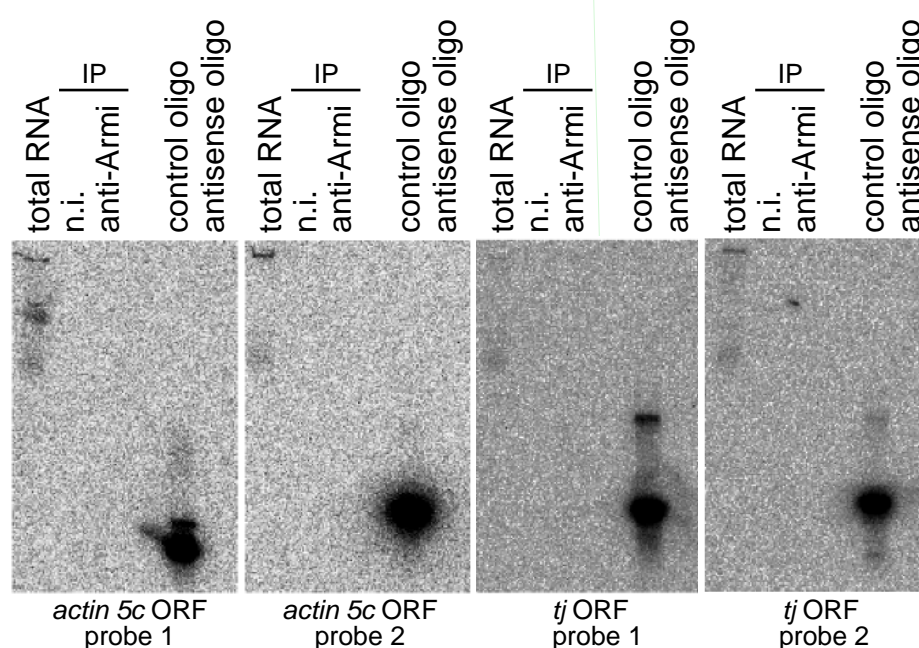


Supplemental Figure S3. (A) Western blotting was performed using anti-Piwi, anti-Armi and anti-Yb antibodies on OSC lysates in which Piwi, Armi and Yb were depleted by RNAi. Anti-Tubulin was used as an internal control. siRNA for *EGFP* was employed as a negative control (control). (B) Depletion of Armi caused Piwi (green) to be mislocalized to the cytoplasm. In contrast, the nuclear localization of TJ protein (red) was unaffected by Armi depletion. (C) Yb depletion causes a severe reduction of the piRNA level in OSCs (~25% of the control signal). (D) The Piwi PAZ mutant (green) (myc-Piwi-PAZmt; containing two mutations, Y327A and Y328A) accumulates in the cytoplasm while myc-Piwi wt (green) localizes to the nucleus, supporting the idea that piRNA loading is required for the nuclear localization of Piwi. DAPI staining (blue) shows the locations of nuclei in the cells. (E) The complexes immunoprecipitated with anti-Yb and anti-Piwi antibodies contain neither AGO1 nor AGO2. (F) Western blot analysis shows that the amounts of Piwi are approximately equal in the complexes immunoprecipitated with anti-Piwi and anti-Armi antibodies only when the anti-Piwi complex was diluted 1:40 before loading.

A

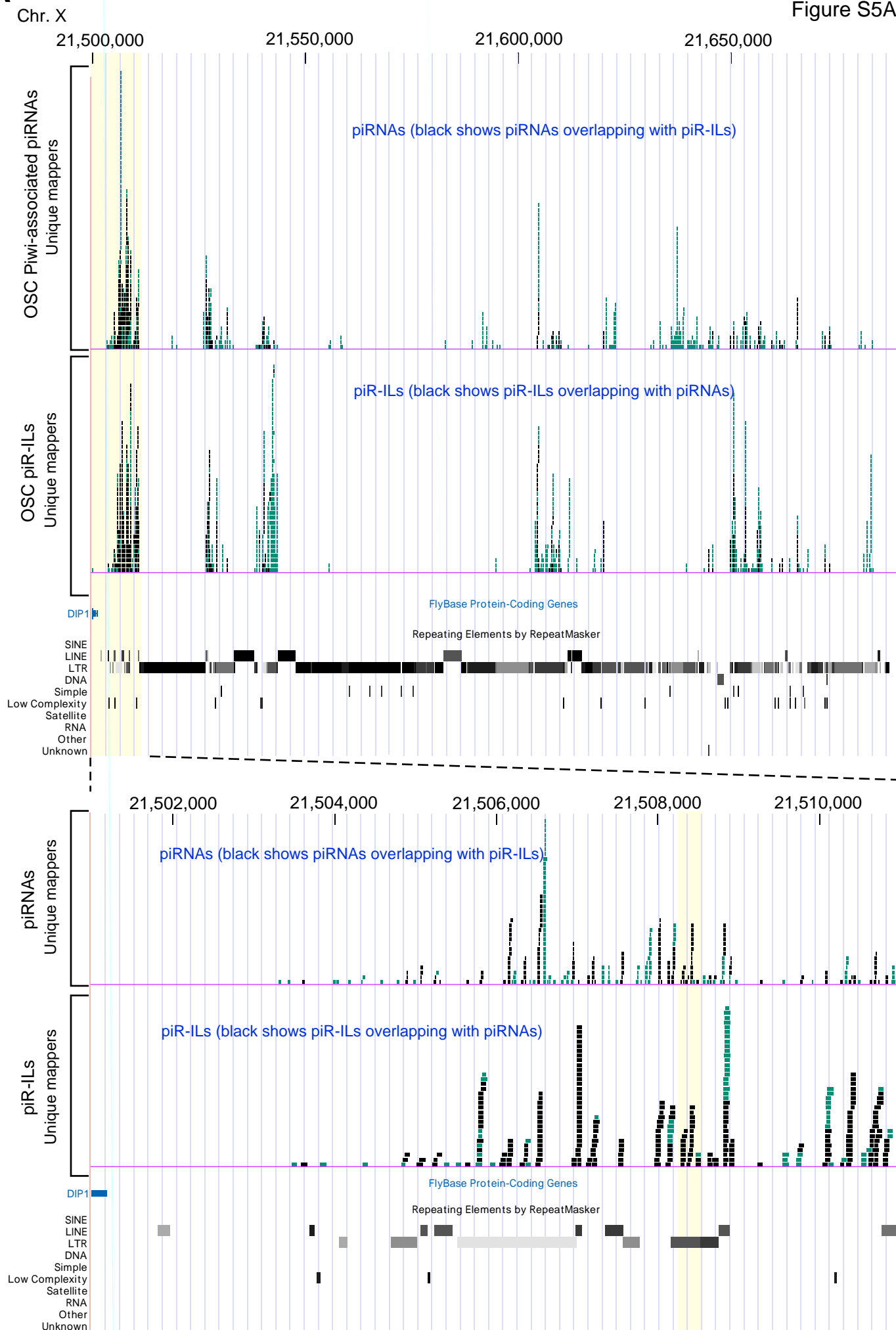


B

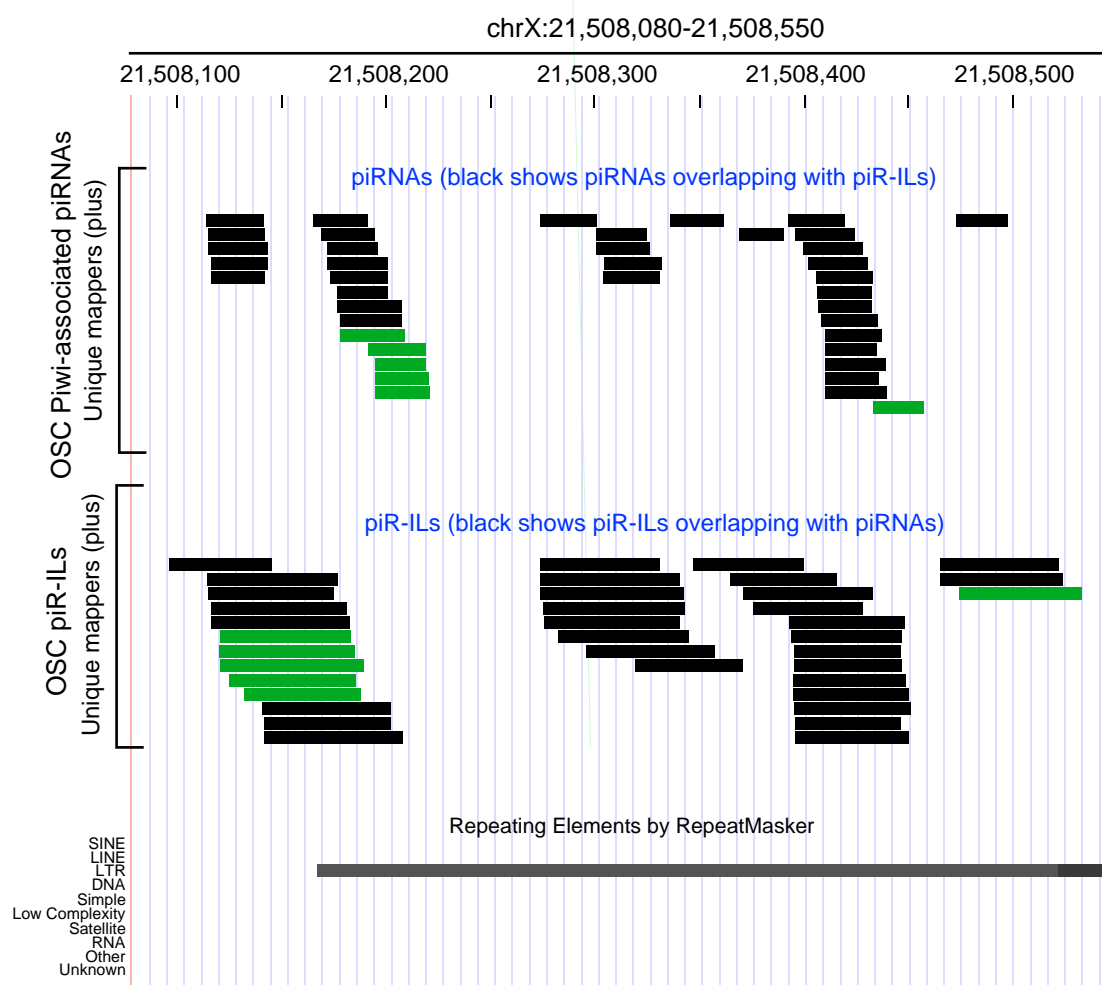


Supplemental Figure S4. piR-IL analyses. (A) The small RNA content (50-75 nt) in the Armi-Piwi-Yb complex perfectly matches the *Drosophila* genome sequence. (B) Northern blotting analyses. RNAs isolated from OSCs (total RNAs) and the anti-Armi immunoprecipitates (anti-Armi IP) were probed with DNA oligos corresponding to *actin 5c* and *tj* ORF. n.i. was used as a negative control for immunoprecipitation. The sequences of the probes used are;
5'-GCCTCGGTCAGCAGCACGGGGTGCT (*actin 5c*-probe1)
5'-CGCAGGATGGCATGGGGAAGGGCAT (*actin 5c*-probe2)
5'-TCAACGTGGTCAGCATGTCGTCATT (*tj*-probe1)
5'-ACCCGAAGCACTACCGTACGAGTTC (*tj*-probe2)
RNAs isolated from the Armi-IP complex appeared negative although control oligos were positive, suggesting that clones corresponding to *actin 5c* and *tj* ORF are background.

A

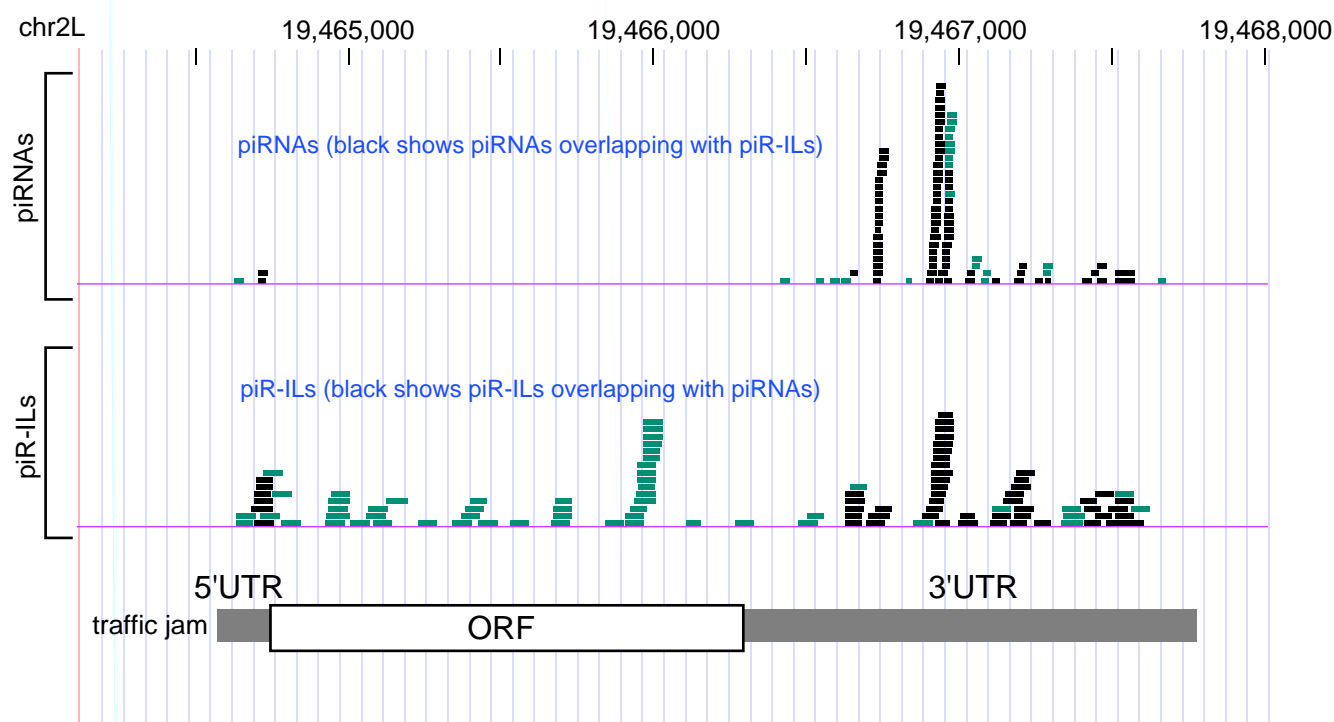


B

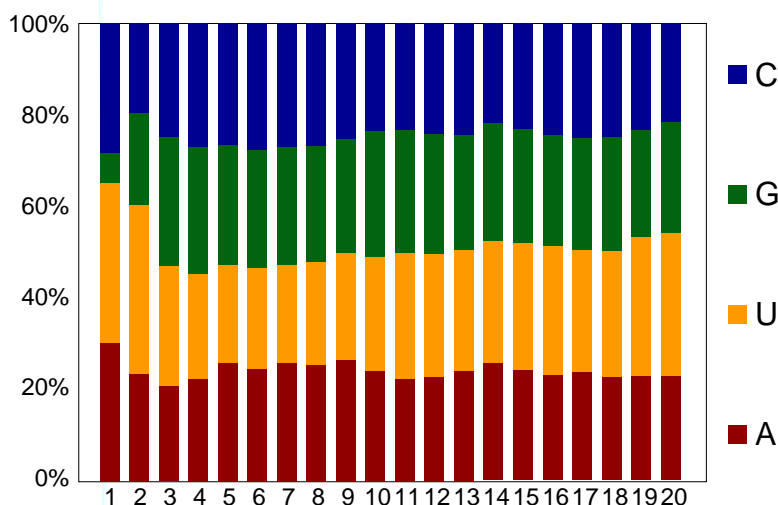


Supplemental Figure S5. (A) Upper: The distribution patterns of piRNAs (Saito et al. 2009) and piR-ILs on the piRNA locus *flam* sequence. Only uniquely mapped ones are shown. Black bars show piRNAs/piR-ILs overlapping with piR-ILs/piRNAs. Green bars show piRNAs/piR-ILs non-overlapping with piR-ILs/piRNAs. Lower: The magnification of the region specified in (A). (B) The distribution of uniquely mapped piR-ILs and mature piRNAs on the chromosome X, position 21,508,080-21,508,550. Black bars show piRNAs/piR-ILs overlapping with piR-ILs/piRNAs. Green bars show piRNAs/piR-ILs non-overlapping with piR-ILs/piRNAs.

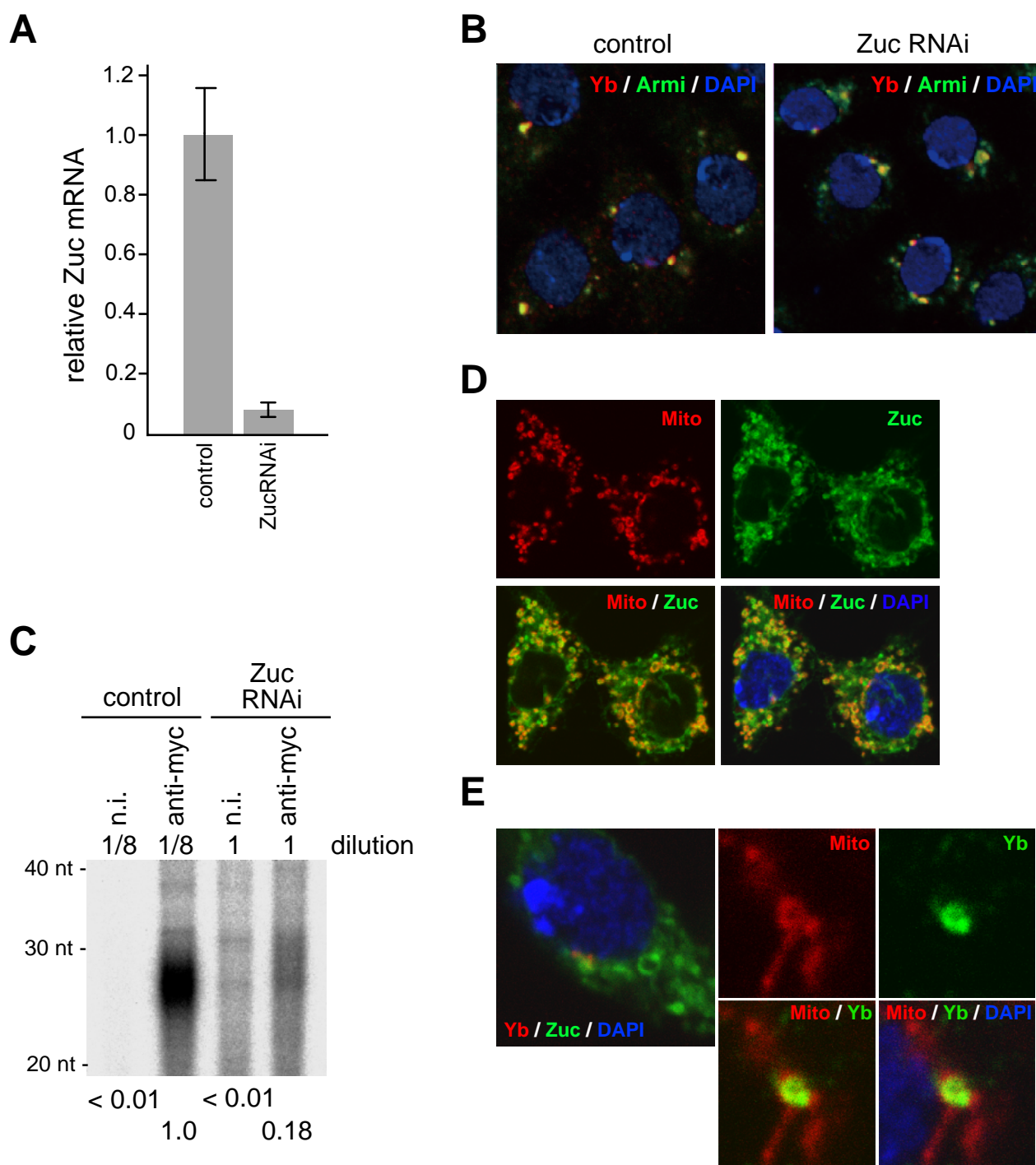
A



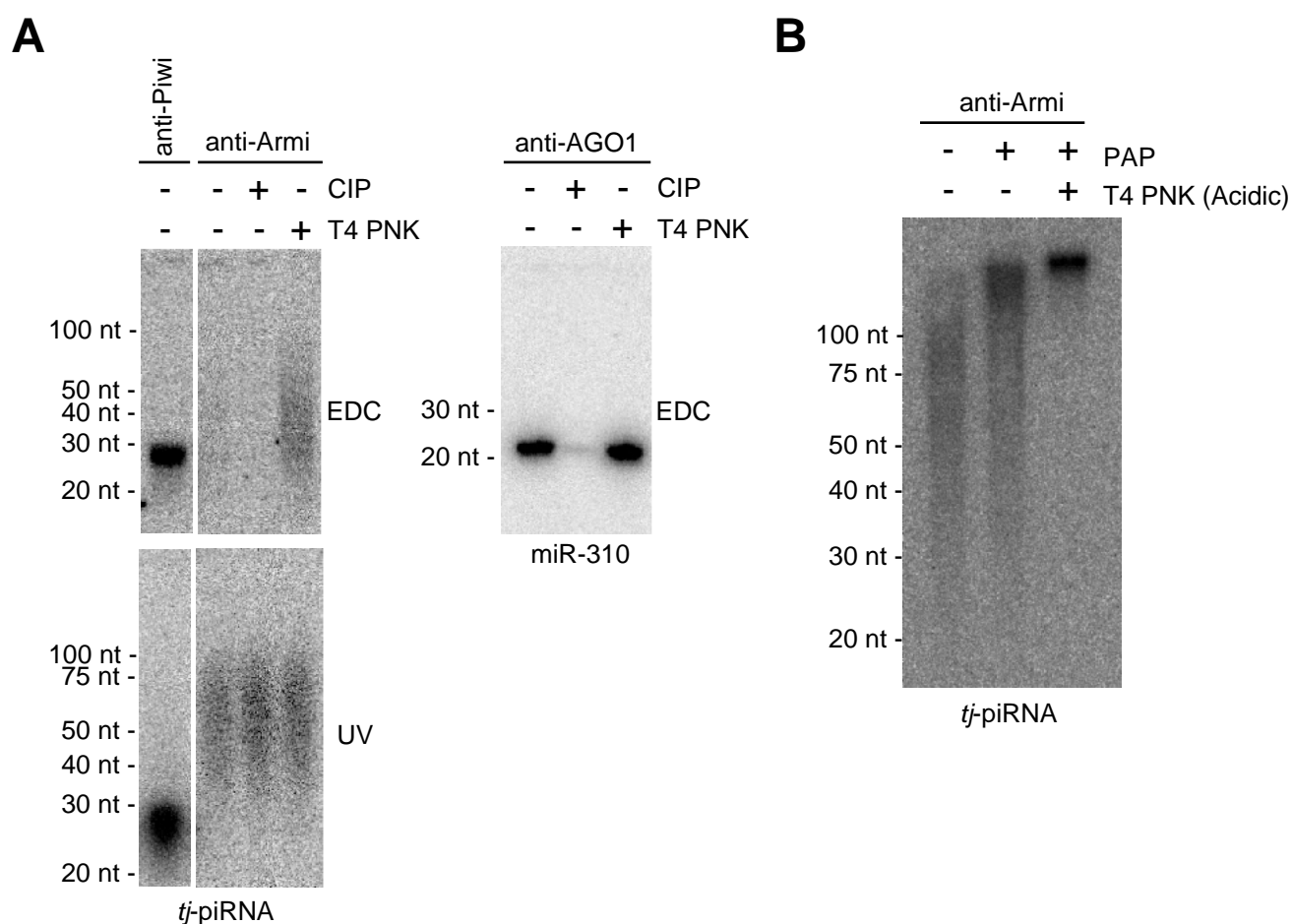
B



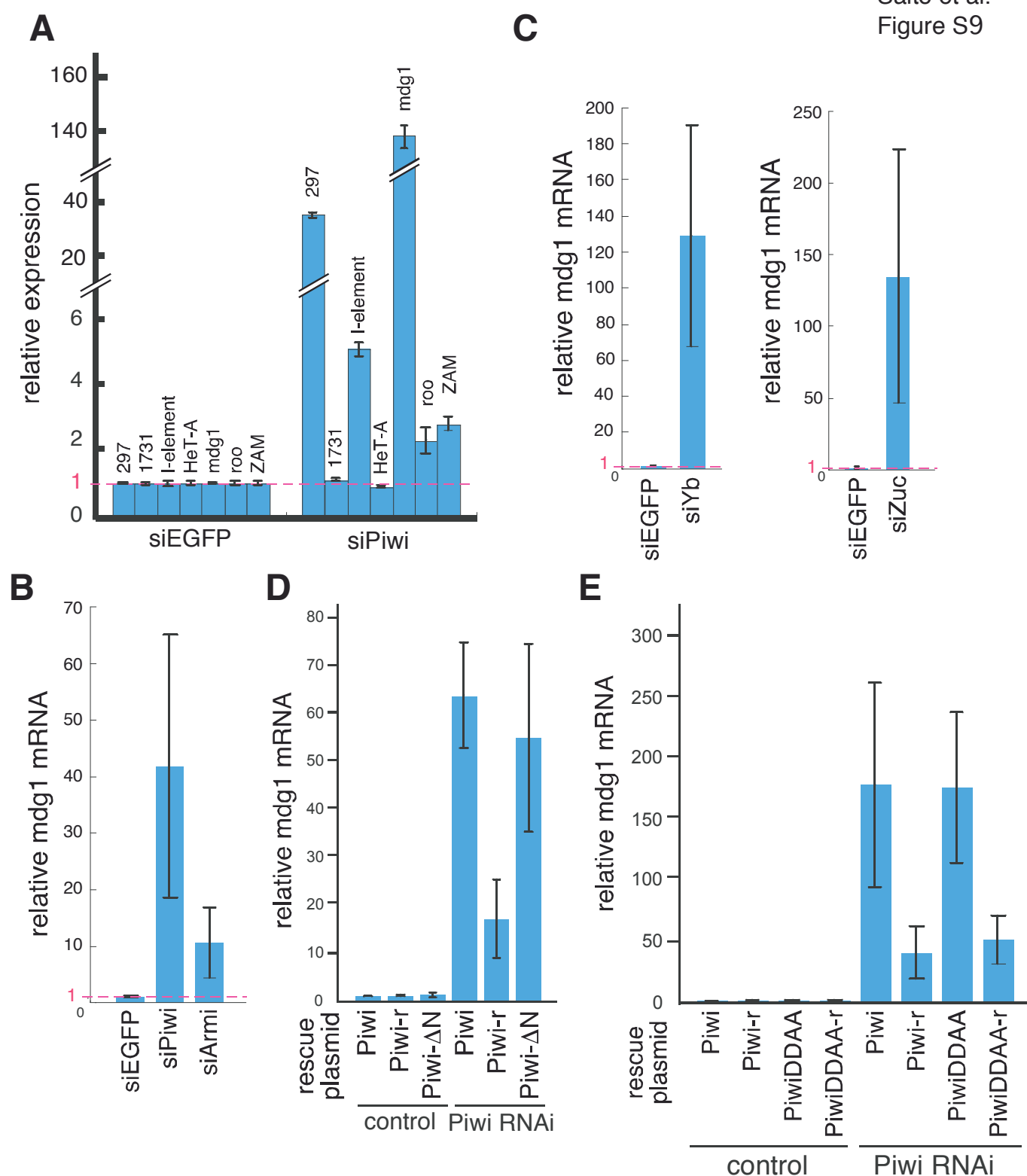
Supplemental Figure S6. (A) The distribution patterns of piRNAs and piR-ILs on the *tj* gene sequence. Some piR-ILs were mapped to the *tj* ORF. However, the signals for the clones were not detected in the Armi-Piwi-Yb complex (Supplemental Fig. S4B) by Northern blotting, suggesting that they may be considered as 'background' of the small RNA library. piR-ILs were detected in the complex by Northern blotting (Fig. 3C and 3D). (B) The 5' end of piR-ILs mapped to transposons was not U-rich as oppose to that of mature transposon-piRNAs. Only a small number of transposn-piR-ILs (~4%) has G at their 5' end, although the reason for this appearance remains unknown.



Supplemental Figure S7. (A) The efficiency of Zuc depletion in OSC was determined by qRT-PCR. (B) Cellular localization of Armi in OSC was not affected by Zuc depletion. (C) ^{32}P end-labeling showed that when Zuc was depleted, myc-Piwi was loaded with far fewer piRNAs compared with loading under normal conditions. (D) Zuc (green) localizes to mitochondria (red) when expressed in OSCs. (E) Left panel; Zuc signals (green) can be detected in close proximity to Yb bodies (red). Right four panels; Yb signals (green) are detected in close proximity to mitochondria (red).



Supplemental Figure S8. (A) piR-ILs are undetectable by northern blotting in which the RNAs were cross-linked by EDC. They become detectable after phosphorylation, suggesting that piR-ILs are free from phosphate groups at both ends. It should be noted that mature *tj*-piRNA and miR-310 are detectable by the EDC method even without phosphorylation. (B) piRNA-ILs are barely polyadenylated unless they were pre-treated with PNK under acidic conditions, suggesting that they contain a cyclic phosphate at their 3' end. From this result, together with those in (A), it is suggested that piR-ILs are free from phosphate groups at 5' end but contain a cyclic phosphate at their 3' end.



Supplemental Figure S9. (A) Piwi depletion in OSCs causes derepression of various transposons. (B) Piwi and Armi depletion by RNAi in OSCs caused derepression of mdg1 transposon. RNAi was performed for 48 hours. (C) Yb and Zuc depletion by RNAi in OSC caused derepression of mdg1. RNAi was performed for 96 hours. (D) Quantitative RT-PCR analysis for the mdg1 transposon. In OSCs where endogenous Piwi was depleted, myc-Piwi-r (RNAi-insensitive Piwi), but not myc-Piwi or myc-Piwi-ΔN (Piwi lacking its nuclear localization signal), was able to rescue transposon derepression. (E) RNAi-insensitive Piwi-r and Piwi-DDAA-r rescued transposon silencing in Piwi-depleted OSC.

Table S1.

Saito et al.

Supplemental Table 1. Genes depleted in OSCs.

Gene	Function	Reference
<i>armi</i>	piRNA pathway	(Vagin et al., 2006; Malone et al., 2009)
<i>mael</i>	piRNA pathway	(Lim and Kai, 2007)
<i>spn-E</i>	piRNA pathway	(Vagin et al., 2006; Malone et al., 2009)
<i>zuc</i>	piRNA pathway	(Malone et al., 2009; Pane et al., 2007; Saito et al., 2009)
<i>dicer1</i>	miRNA pathway	(Vagin et al., 2006)
<i>dicer2</i>	siRNA pathway	(Vagin et al., 2006)

Table S2.

Saito et al.

Supplemental Table 2

Experiment	Primer Name	Primer sequence
Vector construction	Piwi-F	ATAAGCTTGCTGATGATCAGGGACGTG
	Piwi-R	ATAGATCTTTATAGATAATAAACTTCTTTTCGAG
	Piwi-mt-F	CGAGGAGGCACCGCGCAGGGAGGGAGGCCCGCCAGAGCGAAAGC CG
	Piwi-mt-R	CGGGCCTCCCTCCCTGCGCGGTGCCTCCTCGAGAGCTCCTCTCTCT C
	Piwi-PAZmt-F	GATATCAGTTTCGTGGAAGCCGCTCTCACTAAATATAATATACGCATT GCG
	Piwi-PAZmt-R	GCGTATATTATATTTAGTGAGAGCGGCTTCCACGAAACTGATATCTCT ACC
	Myc-tag-5	TCGAGGGAGAGCAGAAACTGATCTCTGAAGAAGACCTGAACTAAG
	Myc-tag-3	GATCCTTAGTTTCAGGTCTTCTTCAGAGATCAGTTTCTGCTCTCCC
	Zuc-F	TTGCTAGCCACCATGTTGATTACCCAAATAATTATGAAACAA
	Zuc-R	ATCTCGAGCTTGAGCTGGATTGGCTCC

Experiment	Gene	Primer sequence (Forward, Reverse)
qRT-PCR	RP49	CCGCTTCAAGGGACAGTATCTG, ATCTCGCCGCAGTAAACGC
	297	CTGGCAAAGGGATTTCATCA, TGCATTCTAAGGCCAAATG
	1731	TATGGGCTGAGGCGATAAAC, CAAGTGGCTCACTGCTGGTA
	I- element	GACCAAATAAAAATAATACGACTTC, AACTAATTGCTGGCTTGTATG
	HeT-A	CGCGCGGAACCCATCTTCAGA, CGCCGCAGTCGTTTGGTGAGT
	Mdg1	AACAGAAACGCCAGCAACAGC, CGTTCCCATGTCCGTTGTGAT
	Roo	CGTCTGCAATGTACTGGCTCT, CGGCACTCCACTAACTTCTCC
	ZAM	ACTTGACCTGGATACACTCACAAC, GAGTATTACGGCGACTAGGGATAC
	Zucchini	TGATTTGGAAGCTGGTGCAG, GCGACACTTGTGGTTTCTGG

Experiment	Gene	Probe sequence
Northern Blot	U6 snRNA	GGGCCATGCTAATCTTCTCTGTA
	miR-310	AAAGGCCGGGAAGTGTGCAATA
	sl-1 esiRNA	GGAGCGAACTTGTTGGAGTCAA
	Tj-piRNA	GGTAATGGGAATGCACTTCTCTTGAA
	Idefix-piRNA	AAACTACTGGCAATCGTTTGGGAA

Experiment	siRNA name	siRNA sense	siRNA antisense
RNAi	EGFP-si	GGCAAGCUGACCCUGAAGUTT	ACUUCAGGGUCAGCUUGCCTT
	Piwi-si	GCUCCCAGGCGUGAAGGUGTT	CACCUUCACGCCUGGGAGCTT
	Zucchini -si	GCAUUGCCGUCAGCACUGUTT	ACAGUGCUGACGGCAAUGCTT
	Armitage-si	CAGCUUAAGGCGAAUCCAATT	UUGGAUUCGCCUUAAGCUGTT
	Yb-si	GGGGUACAUAACCAAGCUTT	AGCUUGGUUGAUGUACCCCTT
	Maelstrom-si	CGCCAAGAUGUCCCAUGAUTT	AUCAUGGGACAUCUUGGCGTT
	Spindle-E-si	CUCGCGGCAUGUAAAGAUUTT	AAUCUUUACAUGCCGCGAGTT
	Dicer1-si	GAUUGUCAUGACAGCGCCGTT	CGGCGCUGUCAUGACAAUCTT
	Dicer2-si	CAGGGAGUGGAUGACUGGATT	UCCAGUCAUCCACUCCUGTT